

## Redundant Kalman Estimation for a Distributed Wireless Structural Control System

R. Andrew Swartz<sup>1</sup> and Jerome P. Lynch<sup>1,2</sup>

<sup>1</sup>Department of Civil and Environmental Engineering

<sup>2</sup>Department of Electrical Engineering and Computer Science  
University of Michigan, Ann Arbor, MI 48109-2125

### Abstract

Eliminating the need for extensive wiring between sensors, actuators and a controller could reduce the cost and enhance the attractiveness of control systems for civil structures. In this study, wireless sensors are proposed for a structural control system with the wireless sensors responsible for the collection of state response data, calculation of control forces, and the issuing of command signals to actuators. While wireless sensors are attractive because of their easy installations, they are limited by the amount of bandwidth available in the wireless communication channel. To address this limitation, the on-board computational resources of wireless sensors are leveraged to alleviate the need for continued use of the wireless channel. Specifically, redundant Kalman state-estimators are encoded in each wireless sensor to estimate the state response of the structure, using only local output measurements. At each time step, the estimated state is compared to the measured system output; when the estimation error exceeds an established threshold, only then is the wireless communication channel used to broadcast updated state information to the remaining wireless sensors. This partially decentralized control method is validated using a 20-story building modeled in a simulation environment. Furthermore, an experimental study is conducted using a three story test structure in which magnetorheological dampers and wireless sensors are installed for the purpose of real-time feedback control during base excitation.

**Keywords:** Wireless sensors, network control, decentralized control, structural control, Kalman estimation

### 1. Introduction

Civil structures subjected to large earthquakes are prone to serious damage and, in rare instances, may collapse. Structural control, first proposed by Yao (1972), is one approach available to the structure engineer to mitigate undesired structural responses. Today, semi-active actuators have been proposed with many actuators defined by compact, power-efficient and low-cost designs (Dyke, *et al.* 1998; Kurata, *et al.* 1999). However, the cost savings offered by today's semi-active devices are often negated by the high costs associated with the installation of the control system. Specifically, the installation of wires needed for communication between sensors, actuators, and a centralized controller can be high. For example, current structural monitoring systems often have installation costs on the order of a few thousand dollars per sensing channel (Celebi 2002). Clearly, eliminating the need for extensive wiring between the nodes of the control system can remove one of the barriers currently impeding the wide-spread implementation of structural control. Real-time feedback control over wireless networks has been shown to be feasible by numerous researchers (Kawka, *et al.* 2004; Ploplys, *et al.* 2004). In previous work, a centralized wireless control scheme for a civil structure using a wireless sensor network was developed and experimentally demonstrated (Wang, *et al.* 2006a). Extensions of this initial study led to the adoption of decentralized control algorithms embedded in the wireless sensor network to eliminate the reliance of the system on raw data transmission (Wang, *et al.* 2006b).

While recent studies exploring wireless sensors applied to structural control have yielded promising results, it is important to emphasize that wireless communication is not a perfect substitute for the more reliable wired communications currently employed. For example, the wireless channel may experience range attenuation, multi-path effects and interference that lead to delays in delivery and loss of data. To address the limitation of potential data loss in a wireless network, send-acknowledgement protocols can be adopted (*e.g.* TCP/IP); however, such protocols slow the effective rate of communication down. To keep the sample rate high, researchers have adopted network protocols where data is transmitted without acknowledgement of receipt (*e.g.* UDP) with the system only taking action (*i.e.* applying control forces) when data is received (Ploplys, *et al.* 2004). In addition to data loss, delays in the delivery of state data can also be a problem in wireless control systems. Horjel (2001) has proposed an approach of closed-loop control for wireless sensor networks where both static and stochastic delays are compensated for by the control algorithm.

Data loss and delay in a wireless sensor network grows faster than at a linear rate as demand for the wireless bandwidth increases. Building on previous work in the fields of network control systems (Yook, *et al.* 2002) and structural control (Seth, *et al.* 2005), this paper will attempt to minimize the probability of data loss and delay by reducing demand for the wireless communication channel. A distributed, partially decentralized control algorithm will be described for implementation in a wireless control system assembled from wireless sensors. The approach will emphasize local computing by each wireless sensor in lieu of automatic use of the wireless communication channel. Specifically, each wireless sensor is programmed to measure its local structural response (*e.g.* interstory velocity). The sensor then uses its

local measurements to estimate the state response of the structure by executing a static Kalman estimator that has been embedded in its computational core. The estimated local state response is compared to that actually measured; if the difference exceeds a predefined threshold, only then is the measured response wirelessly broadcast to the remainder of the wireless sensor network. If an update is received by a wireless sensor, it will automatically update the estimated state vector. The updated state vector is then used by each wireless sensor to determine the control force to be applied to the system by the actuator. This elegant approach to control minimizes the use of the wireless communication channel thereby reducing the probability of delay or loss when state updates are wirelessly transmitted. For validation, a series of shake table tests are conducted using a partial scale three story steel structure in which magnetorheological (MR) dampers and a wireless sensor network are installed for structural control.

## 2. Redundant Kalman Estimation within a Partially Decentralized Control Architecture

A lumped mass shear structure model that analytically describes the lateral response of a building structure subjected to ground motion excitation is proposed. Consider an  $n$  degree-of-freedom structure whose structural properties are described by its mass ( $\mathbf{M}$ ), damping ( $\mathbf{C}'$ ) and stiffness ( $\mathbf{K}$ ) matrices (with dimensions  $n$  by  $n$ ):

$$\mathbf{M}\ddot{\mathbf{z}}(t) + \mathbf{C}'\dot{\mathbf{z}}(t) + \mathbf{K}\mathbf{z}(t) = \mathbf{u}(t) + \mathbf{p}(t) \quad (1)$$

Here,  $\mathbf{z}$ ,  $\mathbf{u}$  and  $\mathbf{p}$  are time-dependent vectors of lateral displacement, control force, and external seismic inertial force applied by the ground motion, respectively. The mass matrix,  $\mathbf{M}$ , is a diagonal matrix whose diagonal terms are the mass of each floor while the stiffness matrix is assembled from the stiffness associated with each floor of the structure :

$$\mathbf{M} = \begin{bmatrix} m_1 & 0 & 0 & 0 \\ 0 & m_2 & 0 & \dots & 0 \\ 0 & 0 & m_3 & & \\ \vdots & & & \ddots & 0 \\ 0 & 0 & 0 & & m_n \end{bmatrix} \quad \mathbf{K} = \begin{bmatrix} k_1+k_2 & -k_2 & 0 & 0 \\ -k_2 & k_2+k_3 & -k_3 & \dots & 0 \\ 0 & -k_3 & k_3+k_4 & & 0 \\ \vdots & & & \ddots & -k_n \\ 0 & 0 & 0 & & k_n \end{bmatrix} \quad (2)$$

The damping matrix,  $\mathbf{C}'$ , is derived assuming Rayleigh damping where the damping coefficient is specified in the first two modes (Chopra 2001). The result is a damping matrix linearly proportional to a sum of the system mass and stiffness:

$$\mathbf{C}' = \alpha_0 \mathbf{M} + \alpha_1 \mathbf{K} \quad (3)$$

To simplify the design process of the optimal control solution, the equation of motion of Equation (1) is converted into a time invariant state space equation where the state variable,  $\mathbf{x}$ , is introduced:

$$\begin{aligned} \dot{\mathbf{x}} &= \mathbf{A}\mathbf{x} + \mathbf{B}\mathbf{u} + \mathbf{E}\mathbf{p} + \mathbf{w} \\ \mathbf{x} &= \{\mathbf{z} \quad \dot{\mathbf{z}}\}^T \end{aligned} \quad (4)$$

The system matrix,  $\mathbf{A}$ , actuator location matrix,  $\mathbf{B}$ , and force location matrix,  $\mathbf{E}$ , can be written:

$$\begin{aligned} \mathbf{A} &= \begin{bmatrix} \mathbf{0} & \mathbf{I} \\ -\mathbf{M}^{-1}\mathbf{K} & -\mathbf{M}^{-1}\mathbf{C}' \end{bmatrix} \\ \mathbf{B} &= \begin{bmatrix} \mathbf{0} \\ -\mathbf{M}^{-1} \end{bmatrix} \quad \mathbf{E} = \begin{bmatrix} \mathbf{0} \\ \mathbf{1} \end{bmatrix} \end{aligned} \quad (5)$$

In the state space representation of the equation of motion (Equation (4)), white process noise,  $\mathbf{w}$ , is included in the model. If it is assumed that velocity meters are installed in the structure, the velocity response of each floor of the structure can be measured. The output response vector of the structure,  $\mathbf{y}$ , assuming velocity meters upon each floor of the structure, can be derived. In the derivation of the output vector, some white noise ( $\mathbf{v}$ ) is included to represent noise inherent in the sensor measurements:

$$\begin{aligned} \mathbf{y} &= \mathbf{C}\mathbf{x} + \mathbf{D}\mathbf{u} + \mathbf{F}\mathbf{p} + \mathbf{v} \\ \mathbf{C} &= [\mathbf{0} \quad \mathbf{I}] \quad \mathbf{D} = [\mathbf{0}] \quad \mathbf{F} = [\mathbf{0}] \end{aligned} \quad (6)$$

An optimal centralized control solution is first formulated for the closed-loop structural control system. Specifically, a linear quadratic regulator (LQR) is selected for implementation in this study. The LQR control solution seeks to find a

reasonable balance between control performance (*i.e.* response mitigation) and control effort (*i.e.* actuation magnitude). Such a balance can be struck by minimizing the cost function,  $J$ :

$$J(\mathbf{u}) = \sum_{k=1}^{\infty} (\mathbf{x}^T[k] \mathbf{Q} \mathbf{x}[k] + \mathbf{u}^T[k] \mathbf{R} \mathbf{u}[k]) \quad (7)$$

The relative weighting between control performance versus control effort can be established by judicious selection of the positive definite matrices  $\mathbf{Q}$  and  $\mathbf{R}$ . In the minimization of the cost function (Equation (7)), the state space equation of motion (Equation (4)) is used to constrain the minimization process using Lagrangian optimization methods. The final result of the optimization process is a linear feedback matrix,  $\mathbf{G}$ , that when multiplied by the state response at time step  $k$ , determines the optimal control force,  $\mathbf{u}[k]$  (Stengle 1994):

$$\mathbf{u}[k] = -\mathbf{G} \mathbf{x}[k] \quad (8)$$

To calculate the optimal control forces, the full state response of the structure is needed. For control systems implemented in practice, a single centralized controller is used to collect the output response vector,  $\mathbf{y}$ , from which the full state,  $\mathbf{x}$ , can be estimated. With the estimated state response, the controller calculates the control forces using Equation (8). The controller then issues actuation commands to the system actuators in order to apply the desired control forces.

In this study, a centralized controller is not used; rather, the control system is implemented upon a network of spatially distributed wireless sensors. The wireless sensors are installed in the structure to make response measurements, wirelessly exchange data with one another, command actuators, and calculate control actions. Unlike tethered counterparts, wireless sensors must be capable of executing their control tasks in the face of potential data delay and data loss common during real-time operation of a wireless communication channel. Furthermore, as demand for the wireless channel increases, the quality of service generally decreases with higher rates of data loss and delay. As a result, the computational resources available at each wireless sensor will be leveraged to alleviate the demand for use of the communication channel at each time step. Specifically, identical Kalman estimators will be embedded in each wireless sensor to predict the full state response of the structure,  $\mathbf{x}[k+1]$ , using the current state response,  $\mathbf{x}[k]$ , and the sensor output of the wireless sensor's degree-of-freedom ( $y_i$ ) at the current time step  $k$ :

$$\mathbf{x}[k+1] = \mathbf{A}_{\text{est}} \mathbf{x}[k] + \mathbf{B}_{\text{est}} y_i[k] \quad (9)$$

The  $\mathbf{A}_{\text{est}}$  and  $\mathbf{B}_{\text{est}}$  matrices of the steady-state Kalman estimator can be written as a function of the discrete-time domain's equation of motion using the discrete time system and actuator location matrices,  $\mathbf{A}_d$  and  $\mathbf{B}_d$ , respectively:

$$\begin{aligned} \mathbf{A}_{\text{est}} &= (\mathbf{A}_d - \mathbf{B}_d \mathbf{G} - \mathbf{L} \mathbf{C} + \mathbf{L} \mathbf{D} \mathbf{G}) \\ \mathbf{B}_{\text{est}} &= \mathbf{L} \end{aligned} \quad (10)$$

Here,  $\mathbf{L}$  is the steady-state Kalman estimator gain matrix. In a fully decentralized control approach, only the steady-state Kalman estimator is needed for each wireless sensor to estimate the full state response. However, the Kalman estimator might not always yield an accurate estimate of the state response. To assess the quality of the Kalman estimator, the error associated with the predicted output response at each wireless sensor degree-of-freedom,  $y_{i,\text{est}}$  is measured:

$$E_i = y_{i,\text{est}}[k] - y_i[k] \quad (11)$$

To compensate for errors associated with the estimation steps, when the estimator error,  $E_i$ , exceeds a predefined threshold, the wireless sensor then broadcasts its true measured output to the remainder of the wireless sensor network. Upon reception of updated state outputs, each wireless sensor updates its estimated state response with true measured state variables. The communication between wireless sensors keeps the state vector estimation bounded within the threshold range established throughout the network. This partially decentralized approach to control can be adjusted by variation of the error threshold used to trigger communication in the wireless sensor network. For example, if the error threshold is set to a value of zero, then a state update is transmitted at every time step by every wireless sensor resulting in a centralized approach to control. Conversely, if the error threshold is set to an infinitely large value, then the error threshold will never be exceeded resulting in a fully decentralized control solution. Clearly, a tradeoff exists between estimator error and communication overhead adjustable by the judicious selection of the error threshold.

### 3. Simulation using 20-Story SAC Benchmark Structure and Semi-Active Dampers

To validate the partially decentralized control method proposed, a numerical simulation is first formulated based on the

20-story benchmark structure included in the 3<sup>rd</sup> generation ASCE Benchmark Control Problem for Seismically Excited Nonlinear Buildings (Ohtori, *et al.* 2004). The benchmark structure implemented in MATLAB was designed as part of the SAC project and is designed to meet building code requirements for the Southern California seismic region. The mass and stiffness values increase toward the base of the structure, as shown in Figure 1. Damping is taken as 5% of critical damping. For this simulation, structural actuators are located on each floor and are assumed to be ideal actuators providing the force required by the control algorithm up to the saturation level of  $\pm 5.0 \times 10^6$  N. In this study, four ground acceleration records are applied at the base of the structure including the El Centro NS 1940 (NS-USGS Station 117), Loma Prieta NS 1989 (Palo Alto SLAC Lab), Kobe EW 1995 (JMA Station), and Sylmar NS 1971 (NS-CDMG Station 24514) earthquake records all normalized to 100 gals peak acceleration. Wireless sensors are placed upon each floor of the structure to record velocity responses and to determine control forces. Based on previous experimental experience with a wireless sensor proposed for structural monitoring applications (Lynch, *et al.* 2006), roughly 2% of the wireless data packets to be transmitted by the wireless sensors are randomly considered lost in transmission during the simulation. Artificial zero-mean Gaussian white-noise with an RMS level of 0.005 m/s is added to the velocity measurements to represent electrical noise in the velocity meters.

Consider the case when the El Centro NS 1940 is applied to the SAC building. The interstory drift response of the 5<sup>th</sup>, 10<sup>th</sup>, 15<sup>th</sup> and 20<sup>th</sup> floor are shown in Figure 2 for three error thresholds. First, an error threshold of 0 m/s is adopted by the wireless sensors. Since there is some finite error always associated with the Kalman estimation, the wireless sensors will transmit their state updates at every time step; this approach is essentially a centralized control architecture where all wireless sensors exchange their state data. In contrast, the error threshold can be set to an infinitely large value. Since this error threshold will never be exceeded, the wireless sensors never exchange their state data resulting in a fully decentralized control architecture. To illustrate the occasional use of the wireless channel by the sensors for updated state information, a third error threshold of 0.01 m/s is selected. As expected, the seismic response of the SAC building is greatest for the case of an infinite error threshold since no state data is exchanged between the wireless sensors. The best level of control performance is attained when the wireless control system adopts a zero error threshold resulting in a centralized configuration. When the error threshold is set to 0.01 m/s, the seismic response of the structure falls between that of the fully centralized ( $E = 0$  m/s) and decentralized ( $E = \infty$  m/s) cases. The maximum peak interstory drift of each floor of the building is plotted in Figure 3 for various error thresholds. Generally, as the error threshold is increased, the mitigation of floor displacements is less effective.

Several cost functions are developed to measure and compare the effectiveness of the control algorithm as the error function varies. Cost functions  $J1$  through  $J6$ , adopted from Ohtori, *et al.* (2004), compare maximum seismic response parameters between the controlled and uncontrolled structure. For example,  $J1$  compares the maximum interstory drift of all the floors during the full time horizon of the seismic excitation:

$$J1 = \frac{\max_{\text{Floor}, t} (|d_{\text{controlled}}|)}{\max_{\text{Floor}, t} (|d_{\text{uncontrolled}}|)} \quad (12)$$

Similarly,  $J2$  and  $J3$  compares the maximum acceleration and base shear respectively:

$$J2 = \frac{\max_{\text{Floor}, t} (|\ddot{z}_{\text{controlled}}|)}{\max_{\text{Floor}, t} (|\ddot{z}_{\text{uncontrolled}}|)} \quad (13)$$

$$J3 = \frac{\max (|\dot{\mathbf{z}}_{\text{controlled}} \mathbf{W}|)}{\max (|\dot{\mathbf{z}}_{\text{uncontrolled}} \mathbf{W}|)} \quad (14)$$

Cost functions  $J4$  through  $J6$  measure the total response of the structure by comparing the vector norm of the controlled interstory drift, acceleration, and base shear time histories to the respective uncontrolled response:

$$J4 = \frac{\text{norm}(|\mathbf{d}_{\text{controlled}}|)}{\text{norm}(|\mathbf{d}_{\text{uncontrolled}}|)} \quad (15)$$

$$J5 = \frac{\text{norm}(|\dot{\mathbf{z}}_{\text{controlled}}|)}{\text{norm}(|\dot{\mathbf{z}}_{\text{uncontrolled}}|)} \quad (16)$$

$$J6 = \frac{\text{norm}(|\ddot{\mathbf{z}}_{\text{controlled}} \mathbf{W}|)}{\text{norm}(|\ddot{\mathbf{z}}_{\text{uncontrolled}} \mathbf{W}|)} \quad (17)$$

Cost function  $J7$  compares the total energy in the system of the controlled and uncontrolled structure:

$$J7 = \frac{\left[ \frac{1}{N} \sum_{i=1}^N \mathbf{x}_i^T \begin{bmatrix} \mathbf{K} & \mathbf{0} \\ \mathbf{0} & \mathbf{M} \end{bmatrix} \mathbf{x}_i \right]_{\text{controlled}}}{\left[ \frac{1}{N} \sum_{i=1}^N \mathbf{x}_i^T \begin{bmatrix} \mathbf{K} & \mathbf{0} \\ \mathbf{0} & \mathbf{M} \end{bmatrix} \mathbf{x}_i \right]_{\text{uncontrolled}}} \quad (18)$$

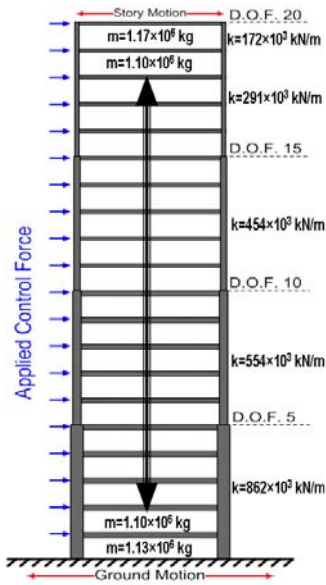


Figure 1. SAC20 benchmark structure.

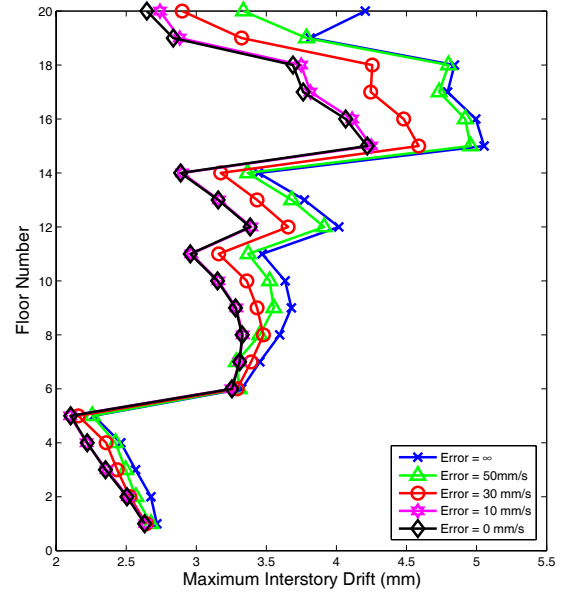


Figure 3. SAC20 benchmark structure maximum interstory drift by floor.

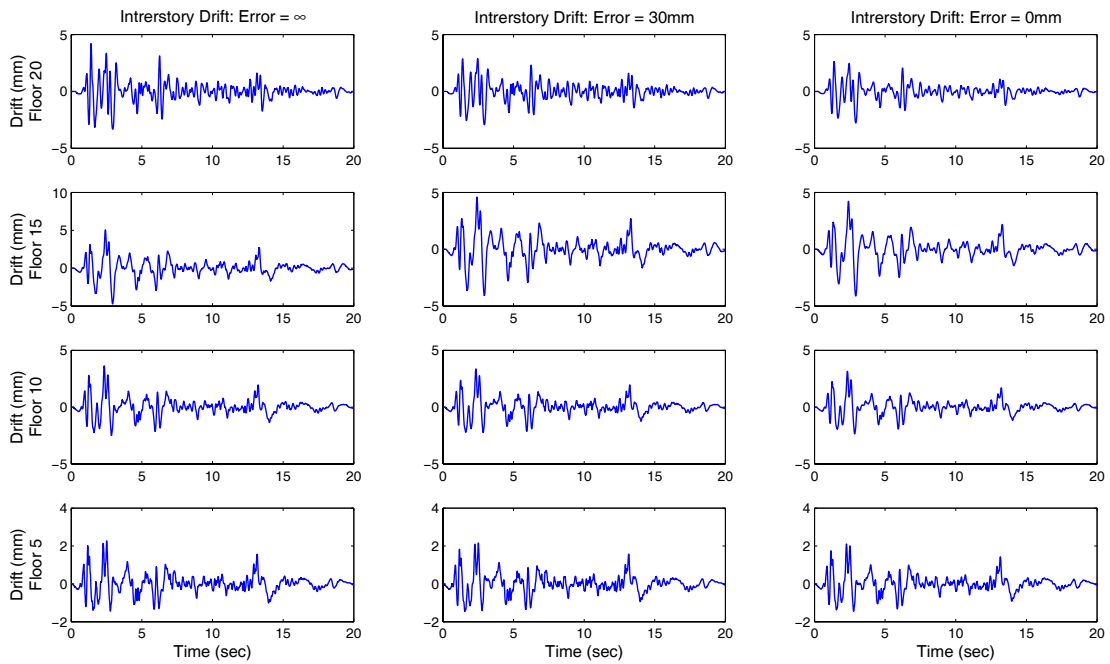


Figure 2. SAC20 benchmark structure interstory drift time history response.

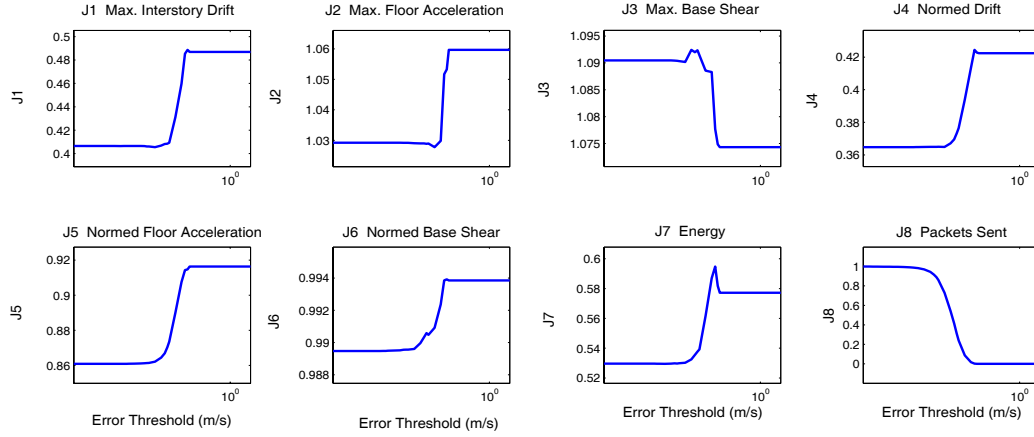


Figure 4. SAC20 benchmark structure cost functions as a function of error threshold.

Finally, cost function  $J8$  measures the number of data transmissions sent during a test normalized by the total number of data transmissions possible during the test:

$$J8 = \frac{(\# \text{ Data Transmissions Sent})}{(\# \text{ Time Steps})(\# \text{ Wireless Units})} \quad (19)$$

The cost functions selected are used to observe the level of performance of the redundant Kalman estimator control system as the error threshold is varied from 0 m/sec to infinitely large values. As shown in Figure 4 for the El Centro NS (100 gal) ground excitation, the performance of the control system, as measured by the eight cost functions, generally decreases in tandem with increases in the error threshold. Only the maximum base shear ( $J3$ ) appears to reduce as the error threshold is increased.

#### 4. Wireless Sensor Prototype for Structural Monitoring and Control: NARADA

The hardware design of a wireless sensor optimized for structural monitoring and control is broken down into four major subsystems. First, a sensing interface is proposed for the collection of data from multiple analog sensors (*e.g.* accelerometers, velocity meters, displacement transducers, strain gages). The primary electrical component employed in the sensing interface is the Texas Instruments ADS8341 16-bit analog-to-digital converter (ADC). The ADS8341 ADC is capable of digitizing analog sensor data (0 to 5V) simultaneously on four channels at sample rates as high as 100 kHz. Second, the computational core is needed to manage sensor data, execute pre-programmed data interrogation tasks, and prepare data for communication. The Atmel 8-bit ATmega128 microcontroller is selected for the computational core because it is low-power consuming less than 100 mW. While the ATmega128 has sufficient on-board memory (128 kB read only memory (ROM)) for the storage of data interrogation algorithms, it lacks sufficient resources for data storage (4 kB of random access memory (RAM)). In response to this limitation, an external static RAM circuit is included in the computational core design. The Cypress CY62128B SRAM component provides 128 kB of RAM for sensor data storage. Third, the wireless interface is used to wirelessly transmit and receive data between nodes of the wireless sensor network. To provide the wireless sensor with the capability to interoperate with other commercial wireless sensor platforms, a wireless transceiver compliant to the IEEE 802.15.4 wireless communication standard is selected. Specifically, the Chipcon CC2420 transceiver, operating on the 2.4 GHz radio band, is selected; this specific radio offers communication ranges in excess of 30 m and data rates as high as 250 kbps. The last subsystem is the actuation interface; this subsystem is intended to allow the wireless sensor to issue voltage signals to structural control actuators. The actuation interface is designed using the Texas Instruments DAC7612 which offers two actuation channels and outputs from 0 to 4V.

After the wireless sensor has been designed, a four layer printed circuit board is designed to house all of the sensor components in a low electrical noise environment. The final printed circuit board is roughly 6 by 6 cm<sup>2</sup> and only 1 cm tall. The Chipcon CC2420 transceiver is self-contained on its own printed circuit board (4 x 3 cm<sup>2</sup>) and plugs into connectors soldered to the wireless sensor's main circuit. The wireless sensor is housed in a hardened container and is powered using 5 AA lithium-ion batteries. A schematic providing the architectural overview of the wireless sensor is presented in Figure 5. The wireless sensor has been named "Narada" after the Javanese messenger of the gods who warns people of

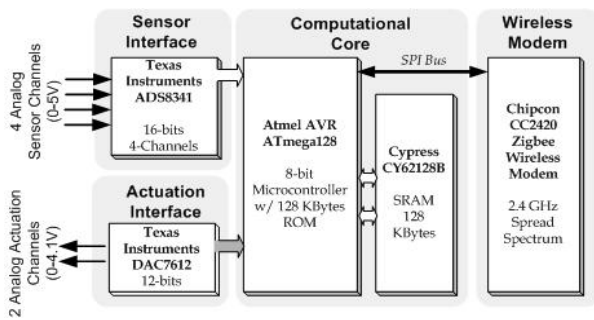


Figure 5. Narada wireless sensor hardware design.

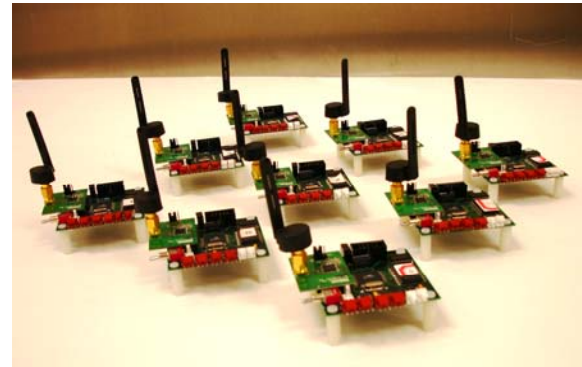


Figure 6. Fully functional Narada wireless sensors.

impending disaster. A picture of a fully functional 9-node network of Narada wireless sensors is presented in Figure 6.

During the design of the wireless sensor, a full implementation of the IEEE 802.15.4 wireless communication protocol stack is implemented in software. This implementation consists of a physical (PHY) layer that operates the physical radio, including channel selection, unit and network identification, and modulation of data on the carrier frequency. In addition to the PHY layer is a medium access control (MAC) layer that defines timing and access to the shared use bandwidth. The MAC layer defined by the IEEE 802.15.4 standard is generally too slow for real-time control applications, requiring approximately 16 ms to transmit a single data packet. Therefore, a special sparse version of the original MAC layer is developed for this study with predefined transmission windows (to avoid collisions) resulting in a much faster, though less adaptable, network capable of transmitting wireless packets in less than 2 ms per transmission.

### 5. Experimental Validation using 3-Story Partial Scale Structure with MR Dampers

To validate the redundant Kalman estimator approach to partially decentralized control of a civil structure, an experimental investigation is undertaken using a partial-scale steel structure base excited by a shaking table. The test structure is a three story steel structure constructed upon a large six degrees-of-freedom shaking table at the National Center for Research on Earthquake Engineering (NCREE), Taiwan. The steel structure is a single bay frame building constructed using I-beam (H150x150x7x10) steel elements. The height of each floor is 3 m (total structure height is 9 m)

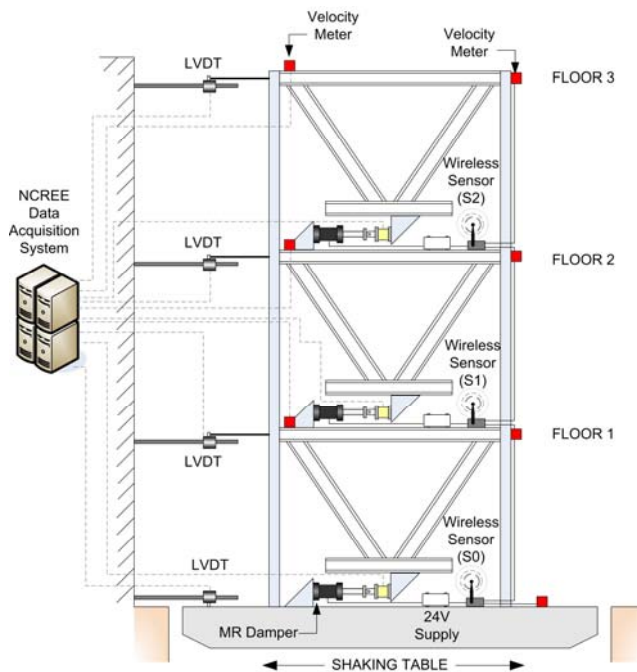


Figure 7. (Left) overview of the wireless control system installed in a 3-story partial scale test structure; (right) the test structure installed upon the NCREE shaking table.

and the area of each floor is 3 by 2 m<sup>2</sup> (Figure 7). Each floor consists of a rigid diaphragm upon which dead weight is added to bring the total floor mass to 6,000 kg. The structure is lightly damped with a damping ratio experimentally determined to be approximately 3% of critical damping.

To control the lateral response of the structure during base excitation, magnetorheological (MR) dampers are installed in the structure. One MR damper is installed upon each floor using V-braces welded to the structure. The MR damper is an academic prototype constructed at NCREE for this study (Lin, *et al.* 2005). The MR damper is of a typical design in which the damper piston is saturated with a silicon oil in which magnetically polarizable particles are suspended. When electrical current is applied to a coil wrapped around the damper cylinder, the resulting magnetic field causes the oil's magnetic particles to align. This alignment transforms the damper fluid into a semi-solid whose yield strength is proportional to the electrical current. The MR dampers are designed to produce a maximum control force of 20 kN and stroke of 10.8 cm. The damping coefficient of the MR damper is adjusted by varying the electrical current applied to the piston coil from 0 to 2 A. Each MR damper is powered by a 24 V power supply. MR dampers are complex semi-active actuators that must be properly modeled before they can be employed within a structural control system. To date, a number of parametric models that relate damper force and shaft velocity have been proposed in the literature (Jung, *et al.* 2005). To model the 20kN MR dampers used in this study, a modified Bouc-Wen model proposed by Lin, *et al.* (2004) is adopted. The model can then be used by each wireless sensor to relate desired control forces to a command voltage to be applied to the MR damper (Lynch, *et al.* 2006).

A wireless control system is installed within the test structure to mitigate its response using MR dampers. One NARADA wireless sensor prototype is installed upon each floor of the structure and labeled as S0, S1 and S2 depending upon the floor it is installed. Each wireless sensor is connected to a voltage-to-current converter supply (VCCS) so that wireless sensor command voltages (0 to 4V) can be converted to a proportional electrical current (0 to 2A) that is then applied to the MR damper. To measure the dynamic response of the structure during base excitation, four Tokyo Sokushin VSE-15-AM servo velocity meters are installed. One velocity meter is installed at each level of the structure (*i.e.* base, 1<sup>st</sup>, 2<sup>nd</sup> and 3<sup>rd</sup> floors). The VSE-15 can measure velocities as large as 1 m/s within a 0.1 to 70 Hz frequency band. With a sensitivity constant of 10 V/(m/s) and a voltage output from -10 to 10V, a signal conditioning circuit is designed to connect the velocity meter to the wireless sensor whose sensor interface is capable of reading only voltage outputs from 0 to 5V. The conditioning circuit shifts the zero mean sensor output to 2.5 V and de-amplifies the meter output by a factor of 4. Each wireless sensor records the output from the velocity meter installed on its floor and from the floor above. This configuration provides each sensor with a direct measurement of the inter-story velocity. In addition to the wireless control system, a tethered data acquisition system native to the NCREE facility is utilized to simultaneously record the response of the test structure. Specifically, linear variable displacement transducers (Temposonics II position sensors) and velocity meters (Tokyo Sokushin VSE-15-AM) are both installed to measure the displacement and velocity response of each story of the test structure. Furthermore, three 50 kN load cells installed in series with each MR damper are interfaced to the tethered data acquisition system to measure the actual control forces applied to the structure.

During a ground excitation, each wireless sensor measures the interstory velocity at its own location and compares that to the estimated value from the previous step (zero, if it is the first step). If the absolute difference is larger than the user defined error threshold, the unit will replace the estimated value for that velocity in the state vector and transmit it during its transmission window. The remaining wireless sensors will receive that measurement and replace the corresponding state estimated value. The wireless sensors are programmed to then calculate the desired control force to be applied by their MR damper using the resulting state vector. Encoded in each wireless sensor is the modified Bouc-Wen model that relates the MR control force to a given command voltage; this model is used to determine the voltage signal the wireless sensor should generate using its actuation interface to command the MR damper (Lynch, *et al.* 2006). This command voltage is then issued to the MR damper by the wireless sensor. The wireless sensors repeat this procedure at each time step for the duration of the ground excitation. When the test is over, test data stored by each wireless sensor (*i.e.* measured interstory velocity, estimated interstory velocity, and desired control force) are transmitted back to a data server for off-line analysis.

Three earthquake ground motions are applied to the test structure during testing (El Centro NS 1940, Kobe EW 1995, Chi-Chi NS 1999). All three ground motions are normalized to a maximum peak ground acceleration of 100 gal. During testing, the wireless sensors are commanded to employ different levels of error thresholding to trigger communication on the wireless channel. Specifically, 7 levels of error threshold are adopted: 0.002, 0.004, 0.008, 0.01, 0.03, 0.04, 0.05 m/s. For each error threshold, the performance of the wireless control system is quantified using cost indices *J1* through *J8*. As shown in Figure 8, the lower error thresholds are more effective in reducing the seismic response of the test structure than higher thresholds. Specifically, the maximum interstory drift (*J1*), maximum base shear (*J3*), and the vector norms of drift (*J4*), acceleration (*J5*), and base shear (*J6*) consistently follow this trend. In tandem to this, the utilization of the wireless communication channel (*J8*) reduces as the error threshold is increased (resulting in greater decentralization).

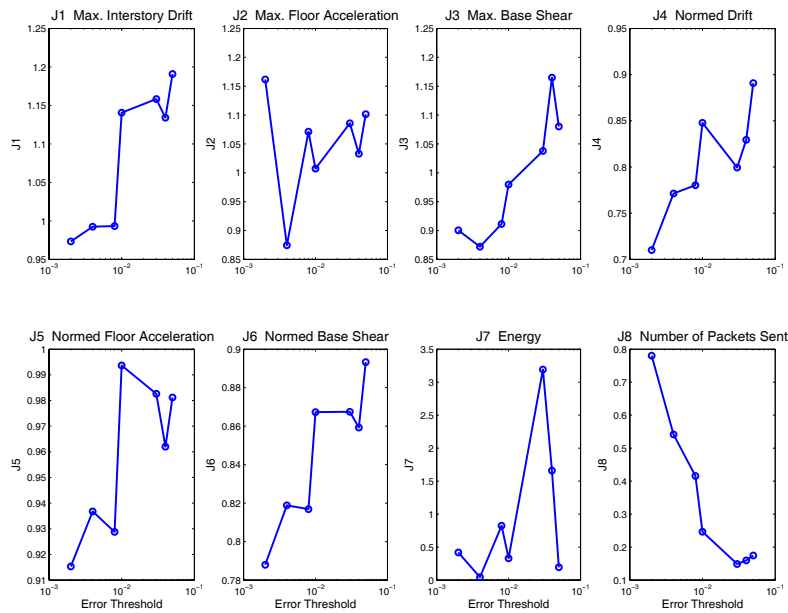


Figure 8. Experimental NCREE structure cost functions for various error thresholds.

## 5. Conclusions

Wireless sensors can be effective when used to sense, compute forces, and actuate in seismic control systems for civil structures. Distributed computing using Kalman estimation can circumvent bandwidth limitations of the control application by eliminating the constant need to transmit raw data between units. By selectively transmitting measured data only when it differs significantly from the estimated data, the available bandwidth can be most effectively leveraged to improve control performance. As the error threshold for transmission increases from zero to effectively infinity, the control performance varies from that of a centralized case to a decentralized case. Additional work focused on different control algorithms is warranted. The effectiveness of LQR control depends on the ability of the wireless sensors and MR dampers to provide the desired control forces; LQR control is sub-optimal when this is not the case. Additionally, further study into performance improvements using adaptive thresholds and hierarchical sensor networks might yield valuable results.

## 6. Acknowledgements

Travel support was provided to the authors by the National Science Foundation for their participation in the US-Korea Workshop for Smart Structures Technology for Steel Structures. The authors would like to express their gratitude to Professors C. H. Loh (NCREE), K. H. Law (Stanford University), and Dawn Tilbury (University of Michigan) for advice and guidance during all facets of the research project.

## 7. References

- Celebi, M. (2002) Seismic Instrumentation of Buildings (with Emphasis on Federal Buildings), Report No. 0-7460-68170, United States Geologic Survey (USGS), Menlo Park, California.
- Chopra, A. (2001) Dynamics of Structures: Theory and Application in Earthquake Engineering, Prentice Hall, Upper Saddle River, NJ.
- Dyke, S. J., Spencer, B. F., Jr., Sain, M. K., and Carlson, J. D. (1998) An Experimental Study of MR Dampers for Seismic Protection, Smart Materials and Structures, Vol. 7, pp. 693-703.
- Horjel, A. (2001) Bluetooth in Control, M.S. Thesis, Dept. of Automatic Control, Lund Institute of Technology, Lund, Sweden.
- Jung, H. J., Spencer, B. F., Ni, Y. Q. and Lee, I. W. (2004) State-of-the-Art of Semi-Active Control Systems Using MR Fluid Dampers in Civil Engineering Applications, Structural Engineering and Mechanics, Vol. 17, No. 3-4, pp. 493-526.

- Kawka, P. A. and Alleyne, A. G. (2004) Stability and Feedback Control of Wireless Networked Systems, Proceedings of the 2005 American Control Conference, Portland, OR, pp. 2953-2959.
- Kurata, N., Kobori, T., Takahashi, M., Niwa, N. and Midorikawa, H. (1999) Actual Seismic Response Controlled Building with Semi-Active Damper System, Earthquake Engineering and Structural Dynamics, Vol. 28, No. 11, pp. 1427-1447.
- Lin, P. Y., Roschke, P. N. and Loh, C. H. (2005) System Identification and Real Application of a Smart Magneto-Rheological Damper, Proceedings of the 2005 International Symposium on Intelligent Control, Limassol, Cyprus.
- Lynch, J. P., Wang, Y., Swartz, R. A., Lu, K. C. and Loh, C. H. (2006) Implementation of a Closed-Loop Structural Control System using Wireless Sensor Networks, Journal of Structural Control and Health Monitoring, submitted.
- Ohtori, Y., Christenson, R. E. and Spencer, B. F. (2004) Benchmark Control Problems for Seismically Excited Nonlinear Buildings, Journal of Engineering Mechanics, Vol. 130, No. 4, pp. 366-385.
- Ploplys N. J., Kawka, P. A. and Alleyne, A. G. (2004) Closed-Loop Control over Wireless Networks, IEEE Control Systems Magazine, pp. 58-71.
- Seth, S., Lynch, J. P. and Tilbury, D. M. (2005) Wirelessly Networked Distributed Controllers for Real-Time Control of Civil Structures, Proceedings of the 2005 American Control Conference, Portland, OR, pp. 2946-2952.
- Stengle, R.F. (1994) Optimal Control and Estimation, Dover Publications, Mineola, NY.
- Wang, Y., Swartz, R. A., Lynch, J. P., Law, K. H., Lu, K. C. and Loh, C. H. (2006a) Wireless Feedback Structural Control with Embedded Computing, Proceedings of the SPIE 11th International Symposium on Nondestructive Evaluation for Health Monitoring and Diagnostics, San Diego, CA.
- Wang, Y., Swartz, R. A., Lynch, J. P., Law, K. H., Lu, K. C. and Loh, C. H. (2006b) Decentralized Civil Structural Control using a Real-Time Wireless Sensing and Control System, Proceedings of the 4th World Conference on Structural Control and Monitoring (4WCSCM), San Diego, CA.
- Yao, J. T. P. (1972) Concept of Structural Control, Journal of Structural Division, ASCE, Vol. 98, No. 7, pp. 1567-1574.
- Yook, J. K., Tilbury, D. M. and Soparkar, N. R. (2002) Trading Computation for Bandwidth: Reducing Communication in Distributed Control Systems using State Estimators, IEEE Transactions on Control Systems Technology, Vol. 10, No. 4, pp. 503-518.